nature geoscience

ARTICLES

https://doi.org/10.1038/s41561-019-0403-x

Global fire emissions buffered by the production of pyrogenic carbon

Matthew W. Jones[1,4*], Cristina Santín[1,2], Guido R. van der Werf[3] and Stefan H. Doerr[1]

Landscape fires burn 3–5 million km² of the Earth's surface annually. They emit 2.2 Pg of carbon per year to the atmosphere, but also convert a significant fraction of the burned vegetation biomass into pyrogenic carbon. Pyrogenic carbon can be stored in terrestrial and marine pools for centuries to millennia and therefore its production can be considered a mechanism for long-term carbon sequestration. Pyrogenic carbon stocks and dynamics are not considered in global carbon cycle models, which leads to systematic errors in carbon accounting. Here we present a comprehensive dataset of pyrogenic carbon production factors from field and experimental fires and merge this with the Global Fire Emissions Database to quantify the global pyrogenic carbon production flux. We found that 256 (uncertainty range: 196–340) Tg of biomass carbon was converted annually into pyrogenic carbon between 1997 and 2016. Our central estimate equates to 12% of the annual carbon emitted globally by landscape fires, which indicates that their emissions are buffered by pyrogenic carbon production. We further estimate that cumulative pyrogenic carbon production is 60 Pg since 1750, or 33–40% of the global biomass carbon lost through land use change in this period. Our results demonstrate that pyrogenic carbon production by landscape fires could be a significant, but overlooked, sink for atmospheric CO_2.

Globally, landscape fires, which include wildfires, deforestation fires and agricultural burns, emit approximately 2.2 Pg C yr^{-1} to the atmosphere (1997–2016)[1]. The majority of this total emission flux is contributed by non-deforestation and non-peatland fire emissions, which are approximately balanced by vegetation regrowth and thus have no net influence on atmospheric stocks of carbon on decadal timescales[2,3]; however, around ~0.4 Pg C yr^{-1} are emitted during tropical deforestation and peatland fires, which contribute to the net global emissions of carbon due to land use change (~1.1–1.5 Pg C yr^{-1} (Fig. 1))[4–6]. These global carbon budget (GCB) estimates are generated by models that represent the temporally distinct processes of immediate carbon emission from burned areas and decadal-scale sequestration through vegetation (re)growth in a spatially explicit manner[1,7,8]. However, such models routinely overlook the coincident flux of biomass carbon to recalcitrant by-products of fire, which can be stored in terrestrial and marine pools for centuries to millennia, and thus provide a long-term buffer against fire emissions (Fig. 1)[9,10–13]. Consequently, the legacy effects of fire that operate on the longest timescales are systematically excluded from models of the carbon cycle and from GCBs[12,14].

These legacy effects are due to the incomplete combustion of vegetation during landscape fires, which transforms part of the remaining organic carbon in the biomass to a continuum of thermally altered products that are collectively termed pyrogenic carbon (PyC)[10,12,15]. The majority of the PyC produced during landscape fires remains initially on the ground in charcoal particles of varying size and is subsequently transferred to its major global stores in soils[16–18], sediments[19,20] and water bodies[21,22]. A smaller fraction of fire-affected vegetation carbon is emitted as PyC in smoke[23,24]. PyC includes labile products of depolymerization reactions as well as aromatic molecules that result from condensation reactions, the latter of which are depleted in functional groups and thus chemically and biologically recalcitrant[25–27]. The enhanced resistance of PyC to biotic and abiotic decomposition leads to its preferential storage in environmental pools[15,20] and a residence time that is typically 1–3 orders of magnitude greater than that of its unburnt precursors[12]. This makes PyC one of the largest groups of chemically discernible compounds in the soil with a contribution to the soil organic carbon stocks of 14% globally[16]. A fraction of the PyC is also conserved across the land-to-ocean aquatic continuum and thus accounts for approximately 10% of riverine dissolved organic carbon[28], 16% of riverine particulate organic carbon[29] and 10–30% of the organic carbon in ocean sediments[13,19,30,31].

A series of reviews and data syntheses have recognized the potential of PyC production to invoke a drawdown (sink) of photosynthetically sequestered CO_2 to pools that are stable on timescales relevant to anthropogenic climate change and its mitigation[9,10,12,13,32–37]. Owing to the relative recalcitrance of PyC, the conversion of biomass carbon to PyC represents an extraction of carbon from a pool cycling on decadal timescales to a pool cycling on centennial or millennial timescales[13,19,20,25,38]. This storage potential contrasts with that of dead vegetation, which degrades on timescales of months to decades or enters soil pools with a shorter residence time than that of PyC[7,11,25,39,40]. Consequently, postfire PyC pools emit carbon to the atmosphere over a significantly longer time period than would be the case in the absence of PyC production and also provide a buffer that moderates atmospheric CO_2 stocks (Fig. 1)[9,12,13]. At present, the fire-enabled vegetation models that are used to make GCB calculations account for short-term fire emissions but routinely exclude fluxes of carbon from biomass to PyC or the delayed emission of carbon from legacy PyC stocks to the atmosphere (Fig. 1)[7,8,14,41,42]. This introduces systematic errors to GCBs through misrepresentation of the effects of modern and historical fires on the exchange of carbon between the atmosphere and terrestrial–marine pools[12–14].

Although PyC has been recognized as a major component of the postfire ecosystem carbon stocks for a number of decades[10,35],

[1]Geography Department, College of Science, Swansea University, Swansea, UK. [2]Biosciences Department, College of Science, Swansea University, Swansea, UK. [3]Faculty of Science, Vrije Universiteit, Amsterdam, Netherlands. [4]Present address: Tyndall Centre for Climate Change Research, University of East Anglia, Norwich, UK. *e-mail: matthew.w.jones@swansea.ac.uk

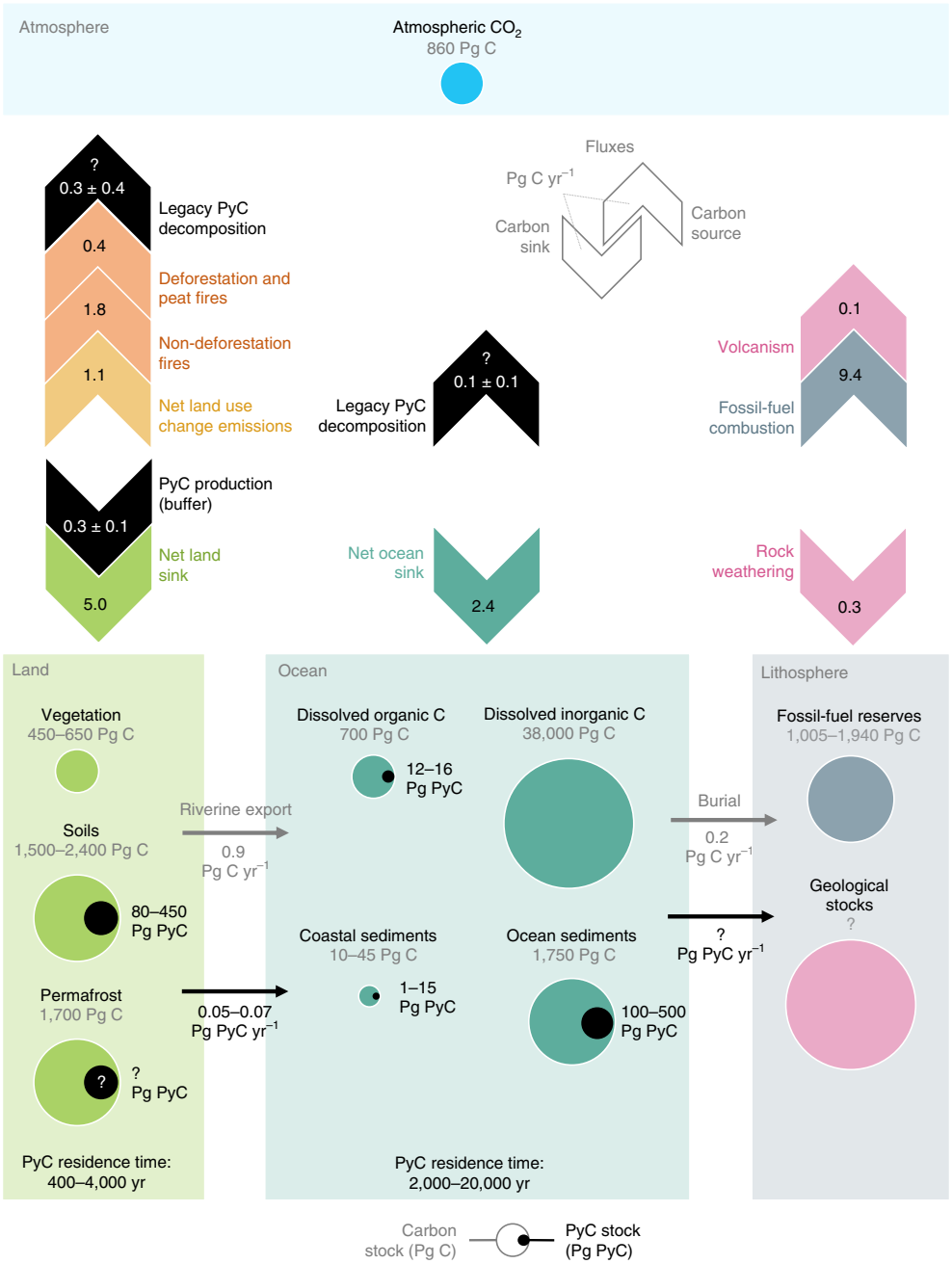

Fig. 1 | Schematic of the global carbon cycle including the buffer and legacy roles of PyC. Stocks (Pg C (1 Pg C = 1×10^{15} g of carbon)) and fluxes (Pg C yr^{-1}) of the global carbon cycle are represented by values from the GCB assessment of the decade 2008–2017[4] and the Intergovernmental Panel on Climate Change fifth assessment report of the decade 2000–2009[6]. Fluxes of carbon due to the net land sink are modified from the GCB to exclude non-deforestation fire emissions, whereas net land use change emissions are modified to exclude deforestation fire emissions. Carbon emissions from deforestation and peat fires and from non-deforestation fires were derived from GFED4s (ref. [1]) and relate to the period 1997–2016. PyC production fluxes due to deforestation and non-deforestation fires are based on estimates from GFED4s+PyC (this study). PyC stocks in soils, ocean dissolved organic carbon and ocean sediments are based on representative PyC/organic carbon ratios in the literature[13,16,68] applied to the estimates of organic carbon stocks and fluxes. PyC fluxes through rivers are the sum of global dissolved and particulate PyC export fluxes[28,29]. Residence times shown for soils derive from a meta-analysis of PyC decomposition in space-for-time substitution studies[69] and incubation experiment estimates extrapolated to field conditions[25]. Residence times for oceanic PyC pools are derived from the literature[19,70]. First-order estimates for legacy PyC decomposition fluxes and their uncertainties are calculated in quadrature for land and ocean pools as the product of the PyC stocks and the reciprocal of the residence times for PyC in these pools, assuming that the low- and high-end estimates for each term represent a consistent portion of normally distributed uncertainty.

quantification of its production rate at the global scale has been problematic and estimates vary by roughly an order of magnitude (50–379 Tg C yr^{-1}) (refs. [12,13,34,36]). A cause of the large range of production estimates is that calculations previously relied on incomplete information regarding the spatial distribution and type of fires, the allocation of carbon among the biomass fuel

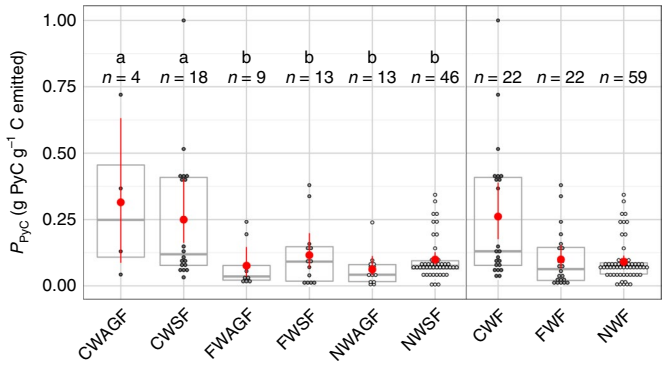

Fig. 2 | The box plots show the distributions of P_{PyC} values for each of the biomass component classes in the production factor dataset. Dots mark the distribution of P_{PyC} values across 1% intervals on the *y* axis. Red dots show the mean P_{PyC} values and red lines show the bootstrapped 95% confidence interval (Methods). Boxes illustrate the median and interquartile range of values. Letters a and b indicate biomass components with statistically similar P_{PyC} distributions at the 95% confidence level according to Tukey honest significant difference tests. The number of data entries (*n*) is also shown. CWF includes both CWSF and CWAGF. CWAGF, coarse woody aboveground fuels; CWSF, coarse woody surface fuels; FWAGF, fine woody aboveground fuels; FWSF, fine woody surface fuels; NWAGF, non-woody aboveground fuels; NWSF, non-woody surface fuels; FWF, fine woody fuels (includes both FWAGF and FWSF); NWF, non-woody fuels (includes both NWAGF and NWSF).

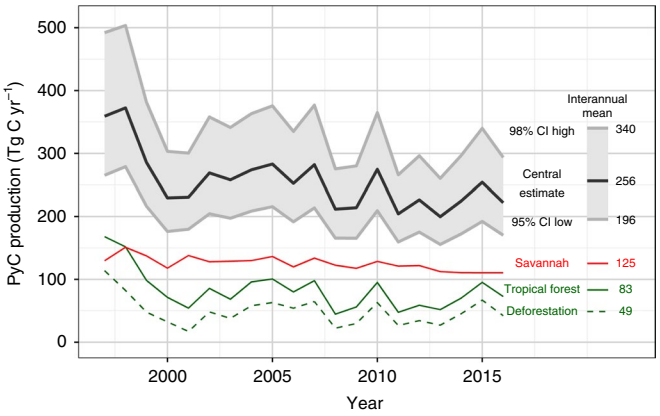

Fig. 3 | Annual global PyC production estimates from GFED4s+PyC for the period 1997–2016. The black line plots the modelled rate of production based on central P_{PyC} ratios (g PyC g^{-1} C emitted) from the global dataset. The shaded area indicates the uncertainty range of the modelled values based on the 95% confidence intervals (CIs) of P_{PyC} values (Fig. 2). The contributions of savannah burning (red line) and tropical forest burning (green solid line) to global PyC production totals are shown, the latter of which includes tropical deforestation fires (green dashed line).

components in burned areas and the specific PyC production factors for these distinct biomass fuel components. To alleviate these issues, we enhanced the Global Fire Emissions Database version 4 with small fires (GFED4s)[1], which is one of the principal process-based models used to make estimates of carbon emission from landscape fires[41,43,44]. Specifically, PyC production was incorporated by following a three-step approach that consisted of: (1) the assembly of the most comprehensive global database of PyC production factors (P_{PyC} (g PyC g^{-1} C emitted)) compiled to date, (2) the assignment of production factors for individual fuel classes stratified as coarse or fine and as woody or non-woody (Fig. 2) and (3) the application of P_{PyC} values to fuel-stratified carbon emissions (grams of C emitted) modelled by the native fuel consumption model in GFED4s. The output is the first global gridded dataset for monthly PyC production at a resolution of 0.25 × 0.25°, covering the years 1997–2016.

Global PyC production

Our central estimate for global PyC production in the period 1997–2016 was 256 Tg C yr^{-1} (Fig. 3), with an uncertainty range of 196–340 Tg C yr^{-1}, which includes variability in the measured P_{PyC} and interannual variability in global production, but excludes uncertainty in GFED4s emissions estimates (Methods). Interannual variability in global PyC production, expressed as the s.d. around the mean, was 47 Tg C yr^{-1} and was most strongly associated with variability in woody fuel combustion, which includes standing wood and coarse woody debris (CWD) (Supplementary Section 1 and Supplementary Fig. 1). Coarse woody fuels (CWF) produce PyC at a greater rate than finer fuels (Fig. 2) and consequently forest fires have disproportionate potential to influence global rates of PyC production (Supplementary Fig. 2).

The El Niño–Southern Oscillation (ENSO) is the primary driver of interannual variability in the burned area in the tropics[45] and previous analyses conducted with GFED showed that carbon emissions from tropical forest ecosystems more than doubled on average during the positive (El Niño) phases relative to the negative (La Niña) ENSO phases[46]. Correspondingly, we calculated that global rates of PyC production in tropical forests were 111% greater during the main fire season of the El Niño phases than during the La Niña phases (Supplementary Table 1). As rates of PyC production by non-forest fires were not sensitive to ENSO (Supplementary Table 1), the major driver of interannual variability in the total PyC production was variability in the tropical forest burned area (Fig. 3). The production of PyC was anomalously high in 1997–1998 (366 Tg C yr^{-1}), which aligns with a particularly strong positive El Niño phase that promoted extensive burning of (tropical) forests in South and Central America and in Southeast and Equatorial Asia[1,46].

Major production regions

The PyC production rates modelled by GFED4s+PyC conformed to a latitudinal pattern (Fig. 4) in which the tropical latitudes clearly dominated production at the global scale. Of the global production, 91% occurred in the tropics and subtropics (0–30° N and 0–30° S), whereas temperate (30–60° N and 30–60° S) and high-latitude (60–90° N) regions provided small contributions to the global total (8% and 1%, respectively).

The global distribution of PyC production also shows intricate regional patterns driven by variation in both the frequency at which fuel stocks were exposed to fire and the magnitude of the fuel stocks that were combusted during the fires that occurred (Supplementary Figs. 3 and 4). Fire frequency was ultimately the key determinant of PyC production rate, which explains why the tropics and subtropics were the dominant source regions. Although savannah fires affect low fuel stocks (Supplementary Section 2), these fires occur frequently and were spatially extensive (Supplementary Fig. 5 and Supplementary Table 2). They thus made the largest contribution to the global PyC production flux (125 Tg C yr^{-1}). Although tropical deforestation fires affected approximately 1% of the area of savannah fires, they affected large stocks of fuel (Supplementary Table 2) and were thus the second largest driver of global PyC production, at 49 Tg C yr^{-1}. The area affected by non-deforestation tropical forest fires was more than a factor of four larger than that of deforestation fires, but fuel consumption was relatively low (Supplementary Table 2). These fires provided the third major component of the global PyC production flux (34 Tg C yr^{-1}). Overall, 81% of the total global PyC production in the period 1997–2016 occurred in savannahs (49%) and tropical forests (32%).

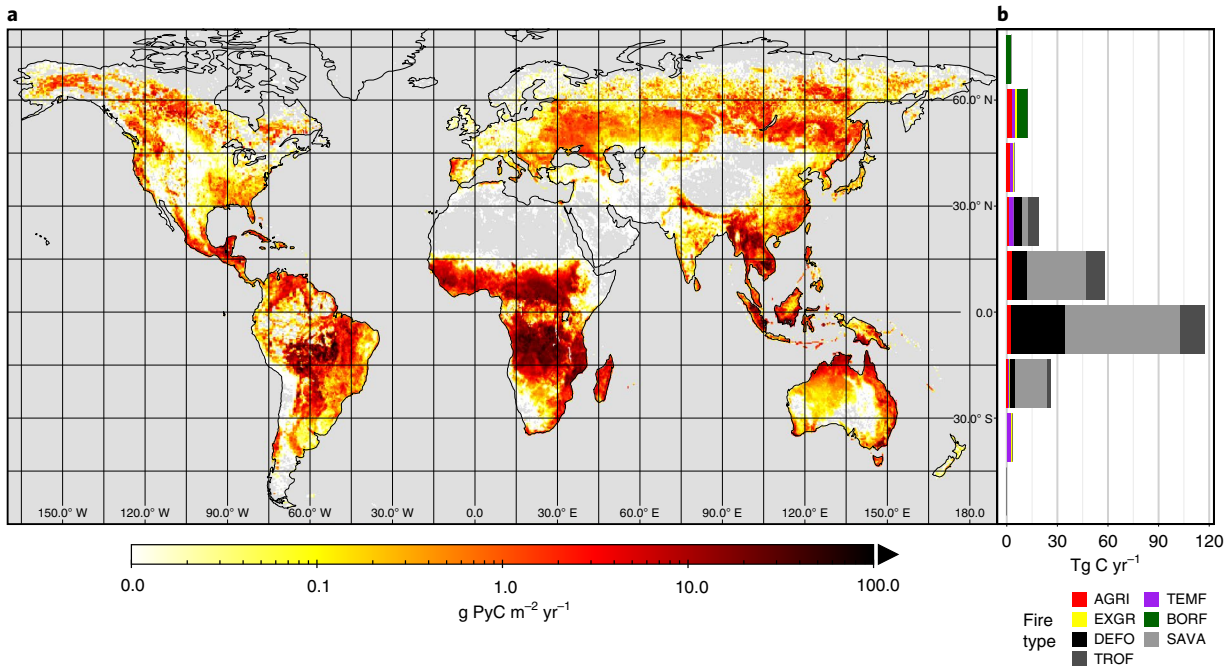

Fig. 4 | Annual average PyC production rates for the period 1997–2016 from GFED4s+PyC, based on central production factors (Fig. 2). a, The average global distribution of PyC production (g C m^{-2} yr^{-1}; note the log scale). **b**, The total production of PyC (Tg C yr^{-1}) in 15° latitudinal bands segregated according to the fire type, which includes savannah fires (SAVA), non-deforestation tropical forest fires (TROF), tropical deforestation fires (DEFO), agricultural fires (AGRI), temperate forest fires (TEMF), extratropical grassland fires (EXGR) and boreal forest fires (BORF).

Global carbon budget implications

Here we have quantified the global gross sink of atmospheric carbon caused by the transfer of photosynthetically sequestered biomass carbon to stocks of PyC during vegetation fires. Our central global PyC production flux estimate (256 Tg C yr^{-1}) is non-trivial within the context of the global carbon cycle (Fig. 1), as it equates to 12% of the global carbon emissions flux due to biomass burning and ~8% of the land sink for atmospheric CO_2 (~3.0–3.2 Pg C yr^{-1}) (refs. [4,6]). The global PyC production flux also equates to 75% of the carbon emitted from tropical deforestation and peat fires, which are the main categories of fire that cause a net loss of carbon to the atmosphere[1,9,47]. The PyC flux modelled here occurs in addition to the smaller global flux of 2 Tg C yr^{-1} caused by the emission of PyC in smoke from vegetation fires (according to equivalent estimates made using GFED4s in the years 1997–2016)[1].

The magnitude of our global estimate for PyC production indicates that the production of PyC during vegetation fires has the potential to significantly influence the atmospheric stock of carbon. A net sink of atmospheric carbon to stocks of PyC can be expected to develop if the flux associated with its production is unmatched by remineralization fluxes from legacy PyC stocks in terrestrial–marine pools (Fig. 1). Earth system models (ESMs) are the most sophisticated tools available to quantify the exchange of carbon between the atmosphere and these pools in time periods for which robust empirical data are sparse or unavailable. Despite previous attempts to highlight the importance of PyC production for carbon storage over timescales relevant to anthropogenic climate change and its mitigation[34,35,48], the absence of the PyC cycle from ESMs has restricted the scope to quantify its role in the carbon cycle[14]. The method introduced here allows for the routine integration of PyC production into fire-enabled vegetation models in a manner that systematically considers the spatial distribution of fire, the composition of the fuel stocks affected and the specific PyC production factors that apply to individual fuel components. This procedure is simple to implement in other fire-enabled vegetation models, which means that the major outstanding challenge to quantifying the net exchange of carbon between the atmosphere and PyC stocks with ESMs is to improve constraints over its storage and residence time in terrestrial and marine pools (Fig. 1)[13,14].

We also show that the PyC cycle must be integrated into ESMs if they are to represent accurately the role of fire in Earth's carbon cycle. The production flux of PyC represents the quantity of carbon that models would otherwise treat either as emitted or as unburned biomass with a residence time in terrestrial pools on the order of months to decades[7,11,25,39,40,49]. At present, the fate of 11% of the global biomass carbon stocks affected annually by fire is misrepresented in global models. As PyC dynamics are not represented in the ESMs used to make GCB calculations[4], this pool may represent a quantitatively significant missing sink or source of carbon to the atmosphere[14,50]. Recent estimates suggest that total carbon emissions from biomass burning in the period 1750–2015 amounted to ~500 Pg C (averaging 1.9 Pg C yr^{-1}) (ref. [41]). Under the assumption that the modern global PyC production flux maintained a constant ratio with the carbon emissions flux throughout this period, we estimate that since the beginning of the industrial revolution ~60 Pg C was transferred to the PyC stocks. This value is equivalent to 33–40% of the carbon lost from biomass pools due to land use change in the same time period (145–180 Pg C) (refs. [6,51]).

Our estimates for the modern and historical PyC production incorporate the best current understanding of PyC production through the combustion of vegetation biomass; however, the limitations of these estimates are worthy of mention. Notably, we do not include the production of PyC through the combustion of organic matter in soils, which may be an important process that drives the accumulation of PyC stocks in environments with deep organic layers, particularly peatlands[52]. We also do not account for the recombustion of PyC in locations that experience secondary burns, which can drive losses of the PyC that remains exposed at the

surface[53]. PyC mass losses through recombustion have been reported as <8% in savannahs[54] and 17–84% in boreal forests[53,55]; however, the long fire return intervals in the latter biome typically allow sufficient time for PyC to be protected from recombustion through its burial in soils[17]. Our exclusion of recombustion is deliberate as we consider the process to be a component of the legacy PyC decomposition flux, which we do not quantify here (Fig. 1). Finally, our dataset of PyC production factors provides values for P_{PyC} that are modulated by fuel class (Fig. 2), but does not take into account fire characteristics (for example, temperature and duration) that are relevant to the formation of PyC[36,56,57]. The continued study of PyC production, with a particular focus on regions with high or rising fire incidence[58–60] and a range of fire intensities[61], will facilitate the application of more specific production factors in spatially explicit global models and thus result in reduced uncertainties in the global PyC production.

The production of PyC may become an increasingly important process for global carbon cycling in future centuries. Although the global burned area has declined in at least the past two decades, due predominantly to the conversion of savannah and grassland to agriculture[62,63], recent fire modelling studies generally agree that this decline is unlikely to continue past the year 2050[58–60]. It is also likely that a higher fraction of global burned area will be distributed in forests in which significant stocks of vegetation carbon are held[58,64,65]. As woody fuels generate more PyC per unit of biomass carbon than other fuels (Fig. 2), the spread of fire into forests can be expected to disproportionately enhance the global PyC production (Supplementary Fig. 2). Although it is less clear how fire prevalence will change in tropical and temperate forests owing to a stronger human control over burning in these regions[58,62], recent increases in fire extent caused by an increasing drought frequency in Amazonia already counteract reductions in the extent of deforestation fires[66]. Notwithstanding the significant uncertainty that exists in model predictions of future fire regimes, there are strong indications that PyC production rates will increase in some of the Earth's most carbon-dense regions in response to a changing climate[7,9,67]. This implies that the buffer for atmospheric CO_2 emissions that results from PyC production will grow in future centuries.

Online content

Any methods, additional references, Nature Research reporting summaries, source data, statements of code and data availability and associated accession codes are available at https://doi.org/10.1038/s41561-019-0403-x.

Received: 22 February 2019; Accepted: 11 June 2019;
Published online: 05 August 2019

References

1. van der Werf, G. R. et al. Global fire emissions estimates during 1997–2016. *Earth Syst. Sci. Data* **9**, 697–720 (2017).
2. Landry, J. S. & Matthews, H. D. Non-deforestation fire vs. fossil fuel combustion: the source of CO_2 emissions affects the global carbon cycle and climate responses. *Biogeosciences* **13**, 2137–2149 (2016).
3. Yue, C. et al. How have past fire disturbances contributed to the current carbon balance of boreal ecosystems? *Biogeosciences* **13**, 675–690 (2016).
4. Le Quéré, C. et al. Global carbon budget 2018. *Earth Syst. Sci. Data* **10**, 2141–2194 (2018).
5. Houghton, R. A. & Nassikas, A. A. Global and regional fluxes of carbon from land use and land cover change 1850–2015. *Glob. Biogeochem. Cycles* **31**, 456–472 (2017).
6. Ciais, P. et al. in *Climate Change 2013: The Physical Science Basis* (eds Stocker, T. F. et al.) 465–570 (Cambridge Univ. Press, 2013).
7. Hantson, S. et al. The status and challenge of global fire modelling. *Biogeosciences* **13**, 3359–3375 (2016).
8. Rabin, S. S. et al. The fire modeling intercomparison project (FireMIP), phase 1: experimental and analytical protocols with detailed model descriptions. *Geosci. Model Dev.* **10**, 1175–1197 (2017).
9. Bowman, D. et al. Fire in the Earth system. *Science* **324**, 481–484 (2009).
10. Kuhlbusch, T. A. J. Black carbon and the carbon cycle. *Science* **280**, 1903–1904 (1998).
11. Lehmann, J. et al. Australian climate–carbon cycle feedback reduced by soil black carbon. *Nat. Geosci.* **1**, 832–835 (2008).
12. Santín, C. et al. Towards a global assessment of pyrogenic carbon from vegetation fires. *Glob. Change Biol.* **22**, 76–91 (2016).
13. Bird, M. I., Wynn, J. G., Saiz, G., Wurster, C. M. & McBeath, A. The pyrogenic carbon cycle. *Annu. Rev. Earth Planet. Sci.* **43**, 273–298 (2015).
14. Landry, J.-S. & Matthews, H. D. The global pyrogenic carbon cycle and its impact on the level of atmospheric CO_2 over past and future centuries. *Glob. Change Biol.* **23**, 3205–3218 (2017).
15. Schmidt, M. W. I. Carbon budget in the black. *Nature* **427**, 305–307 (2004).
16. Reisser, M., Purves, R. S., Schmidt, M. W. I. & Abiven, S. Pyrogenic carbon in soils: a literature-based inventory and a global estimation of its content in soil organic carbon and stocks. *Front. Earth Sci.* **4**, 80 (2016).
17. Ohlson, M., Dahlberg, B., Økland, T., Brown, K. J. & Halvorsen, R. The charcoal carbon pool in boreal forest soils. *Nat. Geosci.* **2**, 692–695 (2009).
18. Koele, N. et al. Amazon Basin forest pyrogenic carbon stocks: first estimate of deep storage. *Geoderma* **306**, 237–243 (2017).
19. Masiello, C. A. & Druffel, E. R. M. Black carbon in deep-sea sediments. *Science* **280**, 1911–1913 (1998).
20. Schmidt, M. W. I. & Noack, A. G. Black carbon in soils and sediments: analysis, distribution, implications, and current challenges. *Glob. Biogeochem. Cycles* **14**, 777–793 (2000).
21. Dittmar, T. & Paeng, J. A heat-induced molecular signature in marine dissolved organic matter. *Nat. Geosci.* **2**, 175–179 (2009).
22. Wagner, S., Jaffé, R. & Stubbins, A. Dissolved black carbon in aquatic ecosystems. *Limnol. Oceanogr. Lett.* **3**, 168–185 (2018).
23. Bond, T. C. et al. Bounding the role of black carbon in the climate system: a scientific assessment. *J. Geophys. Res. Atmos.* **118**, 5380–5552 (2013).
24. Booth, B. & Bellouin, N. Black carbon and atmospheric feedbacks. *Nature* **519**, 167–168 (2015).
25. Kuzyakov, Y., Bogomolova, I. & Glaser, B. Biochar stability in soil: decomposition during eight years and transformation as assessed by compound-specific ^{14}C analysis. *Soil Biol. Biochem.* **70**, 229–236 (2014).
26. Schneider, M. P. W., Hilf, M., Vogt, U. F. & Schmidt, M. W. I. The benzene polycarboxylic acid (BPCA) pattern of wood pyrolyzed between 200 °C and 1000 °C. *Org. Geochem.* **41**, 1082–1088 (2010).
27. Wiedemeier, D. B. et al. Aromaticity and degree of aromatic condensation of char. *Org. Geochem.* **78**, 135–143 (2015).
28. Jaffé, R. et al. Global charcoal mobilization from soils via dissolution and riverine transport to the oceans. *Science* **340**, 345–347 (2013).
29. Coppola, A. I. et al. Global-scale evidence for the refractory nature of riverine black carbon. *Nat. Geosci.* **11**, 584–588 (2018).
30. Lohmann, R. et al. Fluxes of soot black carbon to South Atlantic sediments. *Glob. Biogeochem. Cycle* **23**, GB1015 (2009).
31. Middelburg, J. J., Nieuwenhuize, J. & van Breugel, P. Black carbon in marine sediments. *Mar. Chem.* **65**, 245–252 (1999).
32. Preston, C. M. & Schmidt, M. W. I. Black (pyrogenic) carbon: a synthesis of current knowledge and uncertainties with special consideration of boreal regions. *Biogeosciences* **3**, 397–420 (2006).
33. Goldberg, E. D. *Black Carbon in the Environment: Properties and Distribution* (John Wiley and Sons, 1985).
34. Kuhlbusch, Ta. J. & Crutzen, P. J. Toward a global estimate of black carbon in residues of vegetation fires representing a sink of atmospheric CO_2 and a source of O_2. *Glob. Biogeochem. Cycles* **9**, 491–501 (1995).
35. Santín, C., Doerr, S. H., Preston, C. M. & González-Rodríguez, G. Pyrogenic organic matter production from wildfires: a missing sink in the global carbon cycle. *Glob. Change Biol.* **21**, 1621–1633 (2015).
36. Wei, X., Hayes, D. J., Fraver, S. & Chen, G. Global pyrogenic carbon production during recent decades has created the potential for a large, long-term sink of atmospheric CO_2. *J. Geophys. Res. Biogeosci.* **123**, 3682–3696 (2018).
37. DeLuca, T. H. & Aplet, G. H. Charcoal and carbon storage in forest soils of the Rocky Mountain West. *Front. Ecol. Environ.* **6**, 18–24 (2008).
38. Singh, N., Abiven, S., Torn, M. S. & Schmidt, M. W. I. Fire-derived organic carbon in soil turns over on a centennial scale. *Biogeosciences* **9**, 2847–2857 (2012).
39. Schmidt, M. W. I. et al. Persistence of soil organic matter as an ecosystem property. *Nature* **478**, 49–56 (2011).
40. Thurner, M. et al. Evaluation of climate-related carbon turnover processes in global vegetation models for boreal and temperate forests. *Glob. Change Biol.* **23**, 3076–3091 (2017).
41. Van Marle, M. J. E. et al. Historic global biomass burning emissions for CMIP6 (BB4CMIP) based on merging satellite observations with proxies and fire models (1750–2015). *Geosci. Model Dev.* **10**, 3329–3357 (2017).
42. Yang, J. et al. Century-scale patterns and trends of global pyrogenic carbon emissions and fire influences on terrestrial carbon balance. *Glob. Biogeochem. Cycles* **29**, 1549–1566 (2015).

43. Schultz, M. G. et al. Global wildland fire emissions from 1960 to 2000. *Glob. Biogeochem. Cycles* **22**, GB2002 (2008).
44. Yang, J. et al. Spatial and temporal patterns of global burned area in response to anthropogenic and environmental factors: reconstructing global fire history for the 20th and early 21st centuries. *J. Geophys. Res. Biogeosci.* **119**, 249–263 (2014).
45. Chen, Y., Morton, D. C., Andela, N., Giglio, L. & Randerson, J. T. How much global burned area can be forecast on seasonal time scales using sea surface temperatures? *Environ. Res. Lett.* **11**, 045001 (2016).
46. Chen, Y. et al. A pan-tropical cascade of fire driven by El Niño/Southern Oscillation. *Nat. Clim. Change* **7**, 906–911 (2017).
47. Houghton, R. A. et al. Carbon emissions from land use and land-cover change. *Biogeosciences* **9**, 5125–5142 (2012).
48. Woolf, D., Amonette, J. E., Street-Perrott, F. A., Lehmann, J. & Joseph, S. Sustainable biochar to mitigate global climate change. *Nat. Commun.* **1**, 56 (2010).
49. Surawski, N. C., Sullivan, A. L., Roxburgh, S. H., Meyer, C. P. M. & Polglase, P. J. Incorrect interpretation of carbon mass balance biases global vegetation fire emission estimates. *Nat. Commun.* **7**, 11536 (2016).
50. Santín, C., Doerr, S. H., Preston, C. M. & González-Rodríguez, G. Pyrogenic organic matter produced during wildfires can act as a carbon sink – a reply to Billings & Schlesinger (2015). *Glob. Change Biol.* **24**, e399 (2018).
51. Houghton, R. A. & Nassikas, A. A. Global and regional fluxes of carbon from land use and land cover change 1850–2015. *Glob. Biogeochem. Cycles* **31**, 456–472 (2017).
52. Leifeld, J. et al. Pyrogenic carbon contributes substantially to carbon storage in intact and degraded northern peatlands. *L. Degrad. Dev.* **29**, 2082–2091 (2018).
53. Doerr, S. H., Santín, C., Merino, A., Belcher, C. M. & Baxter, G. Fire as a removal mechanism of pyrogenic carbon from the environment: effects of fire and pyrogenic carbon characteristics. *Front. Earth Sci.* **6**, 127 (2018).
54. Saiz, G. et al. Charcoal re-combustion efficiency in tropical savannas. *Geoderma* **219–220**, 40–45 (2014).
55. Santín, C., Doerr, S. H., Preston, C. & Bryant, R. Consumption of residual pyrogenic carbon by wildfire. *Int. J. Wildl. Fire* **22**, 1072–1077 (2013).
56. Andela, N. et al. The Global Fire Atlas of individual fire size, duration, speed, and direction. *Earth Syst. Sci. Data* **11**, 529–552 (2019).
57. Archibald, S., Lehmann, C. E. R., Gomez-Dans, J. L. & Bradstock, R. A. Defining pyromes and global syndromes of fire regimes. *Proc. Natl Acad. Sci. USA* **110**, 6442–6447 (2013).
58. Knorr, W., Arneth, A. & Jiang, L. Demographic controls of future global fire risk. *Nat. Clim. Change* **6**, 781–785 (2016).
59. Pechony, O. & Shindell, D. T. Driving forces of global wildfires over the past millennium and the forthcoming century. *Proc. Natl Acad. Sci. USA* **107**, 19167–19170 (2010).
60. Flannigan, M. et al. Global wildland fire season severity in the 21st century. *Ecol. Manag.* **294**, 54–61 (2013).
61. Miesel, J., Reiner, A., Ewell, C., Maestrini, B. & Dickinson, M. Quantifying changes in total and pyrogenic carbon stocks across fire severity gradients using active wildfire incidents. *Front. Earth Sci.* **6**, 41 (2018).
62. Andela, N. et al. A human-driven decline in global burned area. *Science* **356**, 1356–1362 (2017).
63. Arora, V. K. & Melton, J. R. Reduction in global area burned and wildfire emissions since 1930s enhances carbon uptake by land. *Nat. Commun.* **9**, 1326 (2018).
64. Flannigan, M. D. et al. Fuel moisture sensitivity to temperature and precipitation: climate change implications. *Clim. Change* **134**, 59–71 (2016).
65. Wang, X. et al. Projected changes in daily fire spread across Canada over the next century. *Environ. Res. Lett.* **12**, 025005 (2017).
66. Aragão, L. E. O. C. et al. 21st century drought-related fires counteract the decline of Amazon deforestation carbon emissions. *Nat. Commun.* **9**, 536 (2018).
67. Krawchuk, M. A. & Moritz, M. A. Burning issues: statistical analyses of global fire data to inform assessments of environmental change. *Environmetrics* **25**, 472–481 (2014).
68. Coppola, A. I., Ziolkowski, L. A., Masiello, C. A. & Druffel, E. R. M. Aged black carbon in marine sediments and sinking particles. *Geophys. Res. Lett.* **41**, 2427–2433 (2014).
69. Singh, B. P., Cowie, A. L. & Smernik, R. J. Biochar carbon stability in a clayey soil as a function of feedstock and pyrolysis temperature. *Environ. Sci. Technol.* **46**, 11770–11778 (2012).
70. Ziolkowski, L. A. & Druffel, E. R. M. Aged black carbon identified in marine dissolved organic carbon. *Geophys. Res. Lett.* **37**, L16601 (2010).

Acknowledgements

This work was funded by a Leverhulme Trust Research Project Grant awarded to S.H.D. (RPG-2014-095), a Swansea University College of Science Fund awarded to M.W.J., a Vici grant awarded to G.R.vdW. by the Netherlands Organisation for Scientific Research (NWO), and a European Union Horizon 2020 research and innovation grant awarded to C.S. (Marie Skłodowska-Curie grant 663830). We thank C. Aponte, C. Boot, G. Clay, G. Cook, F. Cotrufo, P. Fearnside, B. Goforth, R. Graham, M. Haddix, P. Homann, D. Hurst and M. Jenkins for their assistance during the collation of the global dataset of PyC production factors. We also thank B. de Groot for his part in securing funding of the Leverhulme Trust Grant.

Author contributions

M.W.J., C.S. and S.H.D. designed the study. S.H.D. led the Leverhulme Trust Research Project grant that funded the main body of the work. M.W.J. collated the PyC production factor dataset with support from C.S. C.S. and S.H.D. provided unpublished PyC production data. G.R.vdW. provided access to the GFED4s code. M.W.J. adapted the GFED4s code to include PyC production with the support of G.R.vdW. M.W.J. conducted the formal analysis of the production factor dataset and model outputs. All the authors contributed to the interpretation of the results. M.W.J. wrote the manuscript and produced all the figures. All the authors contributed to the refinement of the manuscript.

Competing interests

The authors declare no competing interests.

Additional information

Supplementary information is available for this paper at https://doi.org/10.1038/s41561-019-0403-x.

Reprints and permissions information is available at www.nature.com/reprints.

Correspondence and requests for materials should be addressed to M.W.J.

Publisher's note: Springer Nature remains neutral with regard to jurisdictional claims in published maps and institutional affiliations.

Methods

Global fuel consumption modelling in GFED4s. In GFED4s, carbon emissions to the atmosphere are quantified based on burned area and fuel consumption per unit of burned area. Burned area is derived from satellite data[71] and fires that are too small to be detected by regular burned area algorithms are derived statistically based on active fire detections and relations with, among others, vegetation indices[72]. Fuel consumption is modelled using a satellite-driven biogeochemical model[1] and tuned to match observations[73]. Most of the underlying satellite input datasets have a 500 × 500 m resolution but are aggregated to the model resolution of 0.25° × 0.25°. Total fuel consumption is based on the fuel consumption of several fuel components, which include leaves, grasses, litter, fine woody debris, CWD and standing wood. van der Werf et al.[1] give more information on the GFED4s modelling approach.

To calculate the PyC production within GFED4s we added the production factor P_{PyC}, which quantifies the production of PyC per unit carbon emitted. Until now, the principle obstacle to performing a global modelling exercise of this type was the lack of a sufficiently rich and standardized dataset with which to constrain representative values for P_{PyC}.

Our estimates of uncertainty in the annual PyC production relate only to variability in the PyC production factors and interannual variability in emissions and do not include uncertainties in carbon emission estimates propagate from GFED4s. Uncertainties in GFED4s emissions estimates are discussed at length in van der Werf et al.[1,74] and are predominantly the result of uncertainties in the satellite detection of small fires using thermal anomalies and burn scars. As carbon emissions and PyC production are codependent on the burned area, estimation errors that relate to fire detection introduce scalar uncertainties. Uncertainty in the fuel consumption is an additional component of the overall uncertainty in GFED4s emission estimates[1] and has been reduced from previous versions (for example, GFED3) through its incorporation of a global dataset of fuel consumption estimates[73]. As discussed in the primary literature that relates to the development of the GFED4s[1], a formal global-scale assessment of the uncertainties in fuel consumption cannot be completed due to a paucity of ground truth data for some input datasets. For the previous version of GFED (GFED3), Monte Carlo simulations that accounted for uncertainty in both burned area detection and fuel consumption were used to obtain first-order constraints on the uncertainty in carbon emissions, which were ±20–25% at global, annual scales as a 1 s.d. (1σ) value[74]. Developments of GFED4s included the incorporation of small-fire burned area detection, which led to important reductions in the negative bias in the emissions estimates[72]; however, small fires are also challenging to detect and a lack of validation data prevents the formal investigation of uncertainty in burned area for GFED4s[1,72]. Hence, the true uncertainty of GFED4s is not known precisely, but it is likely to be on the same order as that of GFED3 ($1\sigma = \pm$20–25%). Nonetheless, uncertainty ranges are likely to be greater in regions where small fires are prevalent or where organic soils are affected (for example, Central America, Europe and Equatorial Asia)[1,72].

Regional-scale field studies of fire emissions have served to validate that the GFED modelling framework produces reliable estimates at large scales, for example, in Alaska[75] and the tropics[76]. Studies that involve atmospheric tracers have also provided vital diagnostics for the performance of GFED[1], and generally highlight its proficiency at large scales but reveal some weaknesses in specific regions or during isolated events[77–82]. Overall, GFED4s is highly suited to the investigation of the effects of fire in global-scale biogeochemical cycles and is thus regularly used in GCB assessments[4] and as a reference point for the fire modules of ESMs[7].

Collating a global dataset of PyC production factors. We compiled a new database of P_{PyC} factors (Supplementary Dataset) from a global collection of 22 published studies that reported on PyC production in 91 burn units, as well as two new datasets produced by the authors with 23 burn units reported for the first time here, and we standardized their reporting. All the studies used one of the following two broad approaches to quantify the impacts of fire on the biomass carbon stocks, either prefire and postfire stocks of biomass carbon and PyC are measured or space-for-time substitution is used to constrain burned and unburned stocks of biomass carbon and PyC, which are assumed to be equivalent to prefire and postfire stocks, respectively. Hereafter, the terms 'prefire' and 'postfire' are used to refer to both types of assessment. Here we focus only on PyC present in charcoal and ash[83] on the ground following fire and on charred vegetation. PyC emitted with smoke, transported in the atmosphere and deposited on a regional-scale area is not included as this process has been studied in separate dedicated studies conducted by atmospheric scientists[23] and represents a relatively small flux in comparison (see main text)[12,13].

The P_{PyC} values were calculated for each of the six classes of widely used biomass components: CWSF, which includes CWD or downed wood defined by typical diameter thresholds of >7.6 cm or >10 cm (refs. [84,85]); FWSF, which includes fine woody debris or any other woody debris with diameters below the thresholds for CWSF; CWAGF, which includes trees or branches with diameters greater than the thresholds for CWSF; FWAGF, which includes material described as shrubs, trees or branches with diameters below the thresholds for CWSF; NWSF, which includes litter, understory vegetation, grass, root mat and any other form of non-woody material directly in contact with the ground surface[85,86] and, finally, NWAGF, which includes foliage, leaves, needles, crown fuels and any other forms of non-woody material that attach to standing wood structures above the ground surface.

For each biomass component, P_{PyC} (PyC produced per C emitted) was calculated using the following equation:

$$P_{PyC} = \frac{C_{Py}}{C_{PRE} - C_{POST} - C_{Py}}$$

where C_{Py} is the mass of PyC created during the fire that was attributed to the component, C_{PRE} is the prefire stock of biomass carbon in the component and C_{POST} is the postfire stock of biomass carbon in the unburnt component. C_{Py}, C_{PRE} and C_{POST} are all expressed in the units g C km^{-2}.

Criteria were applied as filters to the dataset to ensure that P_{PyC} could be calculated in a consistent and representative manner. Specifically, P_{PyC} was calculated if the following conditions were met: first, both prefire and postfire biomass stocks were reported and the carbon content (%) was either measured or assumed based on representative values from the literature; second, postfire stocks of pyrogenic organic matter (charcoal, ash and the charred components of partially affected vegetation) were reported and their PyC content (%) was either measured or assumed based on representative values from the literature; third, the type of fire that occurred was representative of a widespread regional fire type (for example, wildfires, slash-and-burn deforestation and prescribed fire) and fourth, in experimental fires, the biomass carbon stock was designed to replicate the density and structure of biomass carbon stocks observed in the field and the burning efficiency was not optimized or adapted as a factor of the study design.

The set of criteria outlined above does not exclude studies that assess the PyC content of charcoal using one of the various chemical or thermochemical techniques available for the separation of PyC from bulk organic carbon[87,88]. Such techniques are frequently used for the detection of PyC in well-mixed soil, sediment and aquatic matrices. However, we note that none of the studies included in our dataset utilized a chemical or thermochemical approach to separate PyC from non-PyC; instead, these studies considered all the organic carbon in residual products of interest (charcoal, ash and the charred components of partially affected vegetation) to be PyC. Thus, we highlight that our estimates of P_{PyC} are free of the intermethod variability in PyC quantification that often confounds the comparison of PyC concentration in environmental matrices across studies and contributes to the notable uncertainty in the magnitude of Earth's major PyC stocks[12,13] (Fig. 1).

Like biomass carbon, total PyC stocks are distributed across several components, which include charcoal and ash on the ground, charcoal attached to CWD and charcoal attached to aboveground vegetation[12]. The majority of the studies included in the production factor dataset matched the studied PyC components to individual biomass carbon components from which they were known to derive. However, as some individual components of the PyC stocks can have a mixture of sources that are indistinguishable from their location or appearance alone, it was occasionally necessary to make assumptions about the biomass components that were sources of these components. This was done on a study-by-study basis. In cases where the source of each PyC component was not explicitly stated, the following procedural steps were adhered to. On a first basis, the PyC component was assigned to a biomass component according to the most probable source inferred, but not explicitly stated, in the primary literature. Second, where more than one biomass component was inferred to be a source of the PyC stock in the primary literature, the PyC stock was weighted proportionally to the prefire stock of carbon present in each of the implicated biomass components. Otherwise, if no sources of PyC were inferred in the primary literature it was necessary to make independent assumptions about the source of PyC in a manner that was consistent with the other studies included in the dataset and our collective experience of quantifying PyC production in the field.

Summary of the production factor values for use in GFED4s+PyC. Our global database suggested that CWSF and CWAGF produce significantly more PyC, relative to carbon emitted, than other fuel classes (their P_{PyC} averaged at 0.25 and 0.31 g PyC g^{-1} C emitted, respectively (Fig. 2)). In contrast, the mean P_{PyC} values for FWSF and FWAGF (0.12 and 0.076 g PyC g^{-1} C emitted, respectively) did not differ significantly from those of NWSF and NWAGF (0.099 and 0.062 g PyC g^{-1} C emitted, respectively). These results are consistent with previous studies, which suggest that large-diameter woody fuels burn less completely and produce PyC in greater proportions than finer fuels[34,35].

For each class, the mean PyC production factor was used as the central estimate for P_{PyC} and the confidence interval around the mean P_{PyC} was calculated through a bootstrapping procedure. Specifically, the available PyC production factors from the dataset were resampled 50,000 times, the mean P_{PyC} was calculated for each resample and the 95% confidence interval was calculated as the middle 95% of the observed 50,000 means (that is, those ranked 1,250th to 48,750th).

According to an analysis of variance with a Tukey honest significant difference post hoc test, no significant differences in mean P_{PyC} were observed between the distributions of P_{PyC} for coarse, fine and non-woody fuels positioned at the ground surface and those same fuels located above the ground surface. Therefore, the

P_{PyC} values applied in GFED4s+PyC are based on the distribution of values in three simplified fuel classes (Fig. 2): CWF (mean 0.26 g PyC g^{-1} C; 95% confidence interval, 0.18–0.39 g PyC g^{-1} C), FWF (mean 0.096 g PyC g^{-1} C; 95% confidence interval, 0.064–0.15 g PyC g^{-1} C) and NWF (mean 0.091 g PyC g^{-1} C; 95% confidence interval, 0.074–0.11 g PyC g^{-1} C).

Assigning PyC production factors in GFED4s+PyC. P_{PyC} values were assigned to each of the native fuel classes of GFED4s[1], which are leaves, grasses, surface fuels (which include litter and fine woody debris), CWD and standing wood (which includes trunks, stems and branches). Mean P_{PyC} values and bootstrapped confidence interval values for CWF, FWF and NWF from the global dataset were used to define representative P_{PyC} values for each of the GFED4s fuel classes (Fig. 2). Full details as to the assignment of P_{PyC} values to each GFED4s fuel class are provided in Supplementary Section 3 and Supplementary Table 3). Briefly, leaf, litter and grass were assigned the relevant P_{PyC} values of NWF, fine woody debris and CWD were assigned the values of FWF and CWF, respectively, and P_{PyC} values for standing wood were applied in a spatially explicit manner as weighted combinations of the P_{PyC} values for CWF (carbon in trunks) and FWF (carbon in branches). The weighted CWF:FWF ratio was assigned according to empirical relationships that defined biomass carbon apportionment to branches and trunks in the various forest types of the GFED4s land cover scheme (Supplementary Section 3 and Supplementary Table 4)[89].

Quantifying ENSO impacts on PyC production. To investigate the influence of pantropical climatic variability driven by the ENSO on the production of PyC, we replicated the analysis presented by Chen et al.[46] with a focus on PyC production rather than on carbon emissions. The pantropics were defined as consisting of Central America, Northern Hemisphere South America, Southern Hemisphere South America, Northern Hemisphere Africa, Southern Hemisphere Africa, Southeast Asia, Equatorial Asia and Australia (Supplementary Fig. 6). The PyC production in El Niño and La Niña phases was compared for the major fire season periods defined in each tropical region by Chen et al.[46]; their study gives a thorough explanation of the rationale for selecting these comparison periods. We summed PyC production in the major fire season period of each region and disaggregated this total to forest and non-forest fires according to the dominant land cover type in the GFED4s land cover scheme (based on the MODIS Land Cover Type Climate Modelling Grid product MCD12C1)[90].

Apportioning sources of PyC. After the GFED4s+PyC model runs, PyC production was assigned to specific sources following a method developed previously for use in GFED4s model runs[1,74]. Specifically, PyC production that occurs as a result of non-deforestation fires was disaggregated in each cell to tropical forest, savannah/grassland, boreal forest, temperate forest and agricultural fires using an existing algorithm that utilizes fractional tree cover, climate and fire-persistence variables. van der Werf et al.[74] give a full discussion of this algorithm. We added an additional latitudinal constraint (30° N to 30° S) to further disaggregate the savannah compartment, which thus separates tropical savannahs and grasslands from extratropical grasslands.

Data availability

The global dataset of the PyC production factors is available as a supplementary data file (GlobalPyC_supplementarydataset.xlsx). This dataset will also be uploaded to the GFED website (http://www.globalfiredata.org) and updated with new data as it becomes available. Supplementary Section 4 contains full references to the studies included in the production factor dataset. Burned area and fire emissions data are publicly available at the GFED website. Additional ancillary data are available from the corresponding author on request.

References

71. Giglio, L., Randerson, J. T. & van der Werf, G. R. Analysis of daily, monthly, and annual burned area using the fourth-generation Global Fire Emissions Database (GFED4). *J. Geophys. Res. Biogeosci.* **118**, 317–328 (2013).
72. Randerson, J. T., Chen, Y., van der Werf, G. R., Rogers, B. M. & Morton, D. C. Global burned area and biomass burning emissions from small fires. *J. Geophys. Res. Biogeosci.* **117**, G04012 (2012).
73. van Leeuwen, T. T. et al. Biomass burning fuel consumption rates: a field measurement database. *Biogeosci. Discuss.* **11**, 8115–8180 (2014).
74. van der Werf, G. R. et al. Global fire emissions and the contribution of deforestation, savanna, forest, agricultural, and peat fires (1997–2009). *Atmos. Chem. Phys.* **10**, 11707–11735 (2010).
75. Veraverbeke, S., Rogers, B. M. & Randerson, J. T. Daily burned area and carbon emissions from boreal fires in Alaska. *Biogeosciences* **12**, 3579–3601 (2015).
76. Andela, N. et al. Biomass burning fuel consumption dynamics in the (sub) tropics assessed from satellite. *Biogeosci. Discuss.* **13**, 3717–3734 (2016).
77. Arellano, A. F., Kasibhatla, P. S., Giglio, L., van der Werf, G. R. & Randerson, J. T. Top-down estimates of global CO sources using MOPITT measurements. *Geophys. Res. Lett.* **31**, L01104 (2004).
78. Hooghiemstra, P. B. et al. Interannual variability of carbon monoxide emission estimates over South America from 2006 to 2010. *J. Geophys. Res. Atmos.* **117**, D15308 (2012).
79. Huijnen, V. et al. Fire carbon emissions over maritime southeast Asia in 2015 largest since 1997. *Sci. Rep.* **6**, 26886 (2016).
80. Castellanos, P., Boersma, K. F. & van der Werf, G. R. Satellite observations indicate substantial spatiotemporal variability in biomass burning NO_x emission factors for South America. *Atmos. Chem. Phys.* **14**, 3929–3943 (2014).
81. Bauwens, M. et al. Nine years of global hydrocarbon emissions based on source inversion of OMI formaldehyde observations. *Atmos. Chem. Phys.* **16**, 10133–10158 (2016).
82. Petrenko, M. et al. The use of satellite-measured aerosol optical depth to constrain biomass burning emissions source strength in the global model GOCART. *J. Geophys. Res. Atmos.* **117**, D18212 (2012).
83. Bodí, M. B. et al. Wildland fire ash: production, composition and eco-hydro-geomorphic effects. *Earth Sci. Rev.* **130**, 103–127 (2014).
84. Hyde, J. C., Smith, A. M. S., Ottmar, R. D., Alvarado, E. C. & Morgan, P. The combustion of sound and rotten coarse woody debris: a review. *Int. J. Wildl. Fire* **20**, 163 (2011).
85. Lutes, D. C., Keane, R. E. & Caratti, J. F. A surface fuel classification for estimating fire effects. *Int. J. Wildl. Fire* **18**, 802 (2009).
86. Sandberg, D. V., Ottmar, R. D. & Cushon, G. H. Characterizing fuels in the 21st century. *Int. J. Wildl. Fire* **10**, 381 (2001).
87. Hammes, K. et al. Comparison of quantification methods to measure fire-derived (black/elemental) carbon in soils and sediments using reference materials from soil, water, sediment and the atmosphere. *Glob. Biogeochem. Cycles* **21**, GB3016 (2007).
88. Zimmerman, A. R. & Mitra, S. Trial by fire: on the terminology and methods used in pyrogenic organic carbon research. *Front. Earth Sci.* **5**, 95 (2017).
89. Thurner, M. et al. Carbon stock and density of northern boreal and temperate forests. *Glob. Ecol. Biogeogr.* **23**, 297–310 (2014).
90. Friedl, M. & Sulla-Menashe, D. *MCD12C1 v006: MODIS/Terra+Aqua Land Cover Type Yearly L3 Global 0.05Deg* (2015); https://doi.org/10.5067/MODIS/MCD12C1.006